THE JOURNAL OF PHYSICAL CHEMISTRY C

Article

pubs.acs.org/JPCC

Structures and Electronic Properties of $V_3Si_n^-$ (n = 3−14) Clusters: A Combined Ab Initio and Experimental Study

Xiaoming Huang,[†] Sheng-Jie Lu,[‡] Xiaoqing Liang,[†] Yan Su,[†] Linwei Sai,[§] Zeng-Guang Zhang,[‡] Jijun Zhao,*[,†] Hong-Guang Xu,*[,‡] and Weijun Zheng[‡]

[†]Key Laboratory of Materials Modification by Laser, Ion and Electron Beams, Dalian University of Technology, Ministry of Education, Dalian 116024, China

[‡]Beijing National Laboratory for Molecular Sciences, State Key Laboratory of Molecular Reaction Dynamics, Institute of Chemistry, Chinese Academy of Sciences, Beijing 100190, China

[§]Department of Mathematics and Physics, Hohai University, Changzhou 213022, China

ABSTRACT: Vanadium-doped silicon cluster anions, $V_3Si_n^-$ (n = 3−14), have been generated by laser vaporization and investigated by anion photoelectron spectroscopy. The vertical detachment energies (VDEs) and adiabatic detachment energies (ADEs) of these clusters were obtained. Meanwhile, genetic algorithm (GA) combined with density functional theory (DFT) calculations are employed to determine their ground-state structures systematically. Excellent agreement is found between theory and experiment. Among the $V_3Si_n^-$ clusters, $V_3Si_5^-$, $V_3Si_9^-$, and $V_3Si_{12}^-$ are relatively more stable. Generally speaking, three V atoms prefer to stay close with others and form strong V−V bonds. Starting from $V_3Si_{11}^-$, cage configurations with one interior V atom emerge.

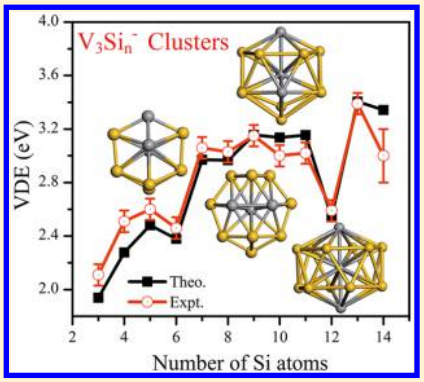

1. INTRODUCTION

As the backbone in modern microelectronics industry, silicon is the most important elementary semiconductor. The continuous trend of miniaturization in microelectronics triggers a quest for nanostructured building blocks. Therefore, there have been tremendous interests in Si nanostructures.[1,2] The research of Si clusters was initiated in the 1980s.[3] It is known that the ground-state configurations of Si clusters strongly depend on cluster size and do not resemble the bulk fragments.[4−8] Silicon clusters prefer to form compact three-dimensional geometries via sp^3 hybridization.[9] Unfortunately, elemental silicon clusters tend to have surface dangling bonds, which renders them chemically reactive and therefore not suitable for nanoscale building blocks.[4] In the past decade, it has been shown both theoretically and experimentally that incorporation of transition metal (TM) atoms into a silicon cluster not only stabilizes the cluster but also brings into peculiar physical properties such as high magnetic moments.[10−19]

Previously, the lowest-energy structures, thermodynamic stabilities, and physical properties of small and medium-sized TM-doped Si_n clusters up to n = 20 have been intensively investigated by ab initio calculations.[10,11,16,20−23] Incorporation of even a single TM atom can lead to stabilization of otherwise unfavorable cage-like silicon structures.[11] The embedding energy of a TM atom (Hf, Zr, Fe, Ru, and Os) is about 12 eV, making the silicon cage stable and compact.[10] Ma et al.[21] showed that Co doping can improve the stability of Si_n clusters when n > 6. Wang et al.[24] discussed the most favorable guest TM atom (TM = Sc−Ni) for Si_{15} and Si_{16} cages and found that $TiSi_n$ have the largest embedding energies and relatively large highest occupied−lowest unoccupied molecular orbital (HOMO−LUMO) gaps.

Particular attentions have been paid to the formation of cage configurations for TM-doped Si_n clusters with different TM elements.[25−29] For 3d TM elements, a perfect metal encapsulation of Si_n cage can be achieved at n = 16, which shows minimum electron affinity and higher stability.[23,25,30,31] It was suggested that VSi_{16}^- is a fluxional endohedral cage, oscillating around a symmetric Frank-Kasper polyhedral transition state,[15] which has also been confirmed in experiments.[12,14] Due to bigger atom radius with regard to 3d TM, 4d TM elements show a different growing pattern with the TM atoms on the exterior region of silicon cluster.[32,33] For instance, in the YSi_n clusters, Y atom either locates at the surface site or acts as a linker between two subclusters when n < 15.[33]

Parallel to the theoretical efforts, there have also been numerous experiments on TM-doped Si_n clusters ($n \leq 20$), including MSi_n (M = Cr, Mn, Cu, Zn) clusters,[12] MSi_{16} (M = Sc, Ti, V),[14] MSi_{16}^- (M = Ti, Zr, Hf),[34] $CrSi_{8-12}$,[35] MSi_n (M = Sc, Y, Ti, Zr, Hf, V, Nb, Ta),[36] MSi_{6-20}^- (M = Sc, Ti, V, Y, Zr,

Special Issue: Current Trends in Clusters and Nanoparticles Conference

Received: November 11, 2014
Revised: December 27, 2014
Published: December 29, 2014

DOI: 10.1021/jp5112845
J. Phys. Chem. C 2015, 119, 10987−10994

Nb),[37] MSi_n (M = Ti, Hf, Mo, W),[38] VSi_{3-6},[39] $VSi_{6-9}^{0,+}$,[40] $CrSin_{3-12}^{-}$,[28] $CuSi_{4-18}^{-}$,[41] $AgSi_{3-12}^{-}$.[42] Mass spectra show that $CrSi_{15,16}^{+}$, $MnSi_{15,16}^{+}$, and $CuSi_{6,10}^{+}$ are particularly abundant, which can be attributed to their endohedral structures.[12] The photoelectron spectra reveal that the electron affinities of MSi_n exhibit local minima around n = 15−16.[38] Koyasu et al.[14,36] systematically doped Si_n clusters with TM atoms of groups 3, 4, and 5 using a double-laser vaporization method. A prominent peak at MSi_{16} was observed in the mass spectra, indicating that species with totally 68 valence electrons are particularly stable. A recent study shows that vanadium atom is doped exohedrally in the silicon clusters and the neutral ones do not differ much from their cationic counterparts.[40]

In contrast to the comprehensive studies on TM-doped Si_n clusters with single metal dopant, as discussed above, little is known about multi-TM doped silicon clusters. Intuitively, incorporation of two or more TM atoms would render the structures and properties of TM_mSi_n clusters ($m \geq 2$) more intriguing. Han et al. have systematically investigated the growth pattern of Mo_2Si_n (n = 9−16) clusters at (U)B3LYP/LanL2DZ level. They showed that cage-like structures are favorable and the Mo atoms prefer to interact with more silicon atoms.[43] Ji and Luo[44,45] systematically studied cage-like M_2Si_{18} (M = Ti−Zn) clusters using DFT calculations. They found that a double hexagonal prism can form when the doped TM atom has no more than half-full d electronic shell. Among all 3d doped M_2Si_{18} clusters, Co_2Si_{18} was the most stable one. Xu et al.[39,46,47] reported a combined study of anion photoelectron spectroscopy (PES) and DFT calculations of small Si_n clusters doped with two vanadium or scandium atoms. Combining experimental PES and DFT-based structural search, we have recently investigated $V_xSi_{12}^{-}$ (x = 1, 2, 3) and found a ferrimagnetic $V_3Si_{12}^{-}$ cluster with wheel-like configuration.[48]

To date, silicon clusters doped with three TM atoms have never been investigated (except for our recent study[48]) within the best of our knowledge. As an embryo of TM−Si alloys, it would be interesting to examine the effects of multiple TM atoms on the atomic and electronic structures of doped Si_n clusters. In particular, determination of the global minimum geometries of TM_3Si_n clusters is a great challenge due to the coexistence of three TM atoms and consequently numerous possible isomer structures on the potential energy surface. Here we perform a combined study of anion PES and DFT-based global search of Si_n clusters (up to n = 14) doped with three vanadium atoms. Vanadium ([Ar] $3d^34s^2$) is chosen as dopant element since it is a 3d transition metal with an open d shell, which results in moderate reactivity and possible magnetism. It would be interesting to explore the interaction between vanadium dopant and silicon host, especially in the cases of coexistence of multiple metal dopants where the interaction between the metal atoms may interplay with the metal−silicon interaction.

2. EXPERIMENTAL AND THEORETICAL METHODS

The experiments were conducted on a home-built apparatus consisting of a laser vaporization cluster source, a time-of-flight mass spectrometer, and a magnetic-bottle photoelectron spectrometer, which has been described elsewhere.[39] The V−Si cluster anions were generated in the laser vaporization source by laser ablation of a rotating translating disk target (13 mm diameter, V/Si mole ratio 1:2) with the second harmonic of a nanosecond Nd:YAG laser (Continuum Surelite II-10). The typical laser power was about 10 mJ/pulse. With ∼4 atm helium gas, backing pressure was allowed to expand through a pulsed valve (General Valve Series 9) into the source to cool the formed clusters. The generated cluster anions were mass-analyzed with the time-of-flight mass spectrometer. The cluster anions of interest were size-selected with a mass gate, decelerated by a momentum decelerator, and crossed with the beam of an Nd:YAG laser (Continuum Surelite II-10, 266 nm) at the photodetachment region. The electrons from photodetachment were energy-analyzed by the magnetic-bottle photoelectron spectrometer. The resolution of the magnetic-bottle photoelectron spectrometer was about 40 meV at electron kinetic energy of 1 eV. The photoelectron spectra were calibrated with the spectra of Cu^- and Au^- ions taken at similar conditions.

Theoretically, the low-lying structures of $V_3Si_n^-$ (n = 3−14) cluster anions were globally searched using genetic algorithm[49,50] incorporated with DFT calculations (GA-DFT). In the GA search, 24 initial configurations in the population were generated randomly. During each GA iteration, any two individuals were chosen as parents to produce a child cluster,[50] followed by an optional mutation operation of 50% probability. Three types of mutation operations were adopted here: (1) exerting each atom a small random displacement, (2) moving several selected atoms by small step and keeping other atoms fixed, and (3) exchanging the atomic types of two heteroatoms. The child cluster was then fully relaxed by DFT optimization without symmetry constraint, using DMol^3 program[51,52] with double numerical basis including d-polarization function (DND) and the Perdew-Burke-Enzerhof (PBE) functional within generalized gradient approximation (GGA).[53] Self-consistent field calculations were done with a convergence criterion of 10^{-6} Hartree on the total energy and real-space orbital cutoff of 6.5 Å. The optimized child cluster may enter the population if it has lower energy than an existing member. The diversity of the GA population was ensured by distinguishing the identical configurations in terms of their inertia.[54] For each cluster size, we performed more than 2000 GA iterations to reach global minimum on the potential energy surface. The validity and efficiency of the present GA-DFT scheme have been well demonstrated in our previous studies on Ga_n,[55] Na_n,[56] Na−Si,[54] $(WO_3)_n$,[57] and AuAg[58] clusters. As a successful application, the most stable configurations of neutral and anionic Na_nSi_m (n = 1−3, m = 1−11) clusters were obtained and the theoretical electronic properties compare well with experimental data.[54]

The accuracy of the present DFT methodology was assessed by benchmark calculations for V_2 and Si_2 dimers as well as bulk solids of V and Si. Upon spin-polarized DFT calculation, the V_2 dimer has 1 μ_B magnetic moment on each V atom. The calculated V−V bond length (BL) is 1.798 Å, in excellent agreement with experimental value of 1.77 Å.[59] Similarly, the theoretical Si−Si BL of 2.175 Å is comparable to 2.246 Å in experiment.[60] From our DFT calculations, the vibrational frequencies for V_2 and Si_2 dimers are 615.9 and 532.1 cm^{-1}, which compare reasonably with experimental data of 537 cm^{-1}[59] and 510.98 cm^{-1},[60] respectively. For reference, previous theoretical results of bond length and frequency for V_2 dimer were 1.797 Å and 630.5 cm^{-1} at BLYP/DND level.[44] The calculated ionization energies of V_2 and Si_2 dimers are 6.549 and 7.823 eV, which are also in line with the experimental data of 6.357 eV[61] and 7.9 eV,[62] respectively. On the other hand, from our calculations, the lattice parameters for silicon (in diamond structure) and vanadium (in bcc structure) solids are

DOI: 10.1021/jp5112845
J. Phys. Chem. C 2015, 119, 10987−10994

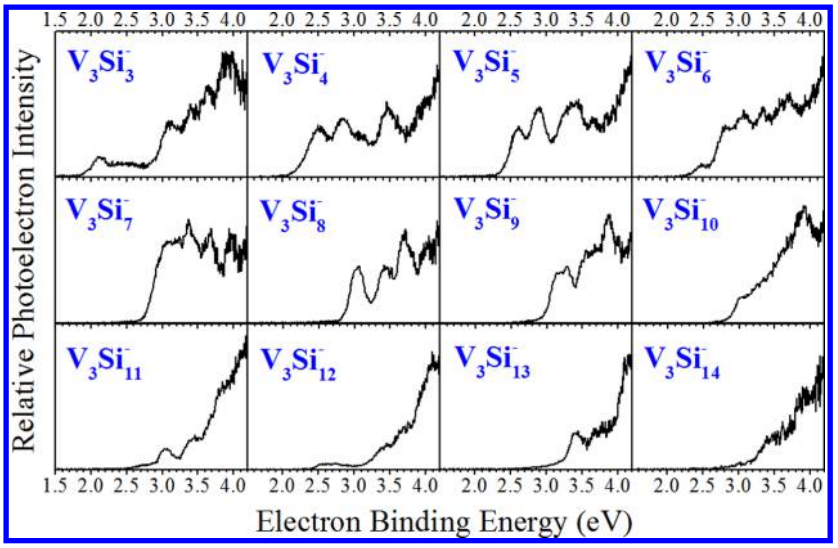

Figure 1. Photoelectron spectra of $V_3Si_n^-$ clusters (n = 3−14) recorded with 266 nm photons.

Table 1. Data of Experimental and Theoretical Vertical Detachment Energies (VDEs) and Adiabatic Detachment Energies (ADEs), Binding Energies (E_b), Second-Order Energy Differences (Δ_2E), HOMO-LUMO Gaps of $V_3Si_n^-$ Clusters are Shown in the Unit of eV

	VDE		ADE				
cluster	expt.	theo.	expt.	theo.	E_b	Δ_2E	gap
$V_3Si_3^-$	2.11 ± 0.08	1.94	1.90 ± 0.08	1.76	3.59		0.83
$V_3Si_4^-$	2.51 ± 0.08	2.28	2.14 ± 0.08	2.18	3.75	0.043	1.07
$V_3Si_5^-$	2.60 ± 0.08	2.48	2.34 ± 0.08	2.38	3.86	0.063	0.78
$V_3Si_6^-$	2.46 ± 0.08	2.38	2.18 ± 0.08	2.36	3.91	−0.013	0.61
$V_3Si_7^-$	3.06 ± 0.08	2.97	2.73 ± 0.08	2.75	3.98	0.021	0.93
$V_3Si_8^-$	3.03 ± 0.08	2.97	2.81 ± 0.08	2.89	4.03	−0.004	0.75
$V_3Si_9^-$	3.15 ± 0.08	3.16	2.96 ± 0.08	3.08	4.07	0.057	0.91
$V_3Si_{10}^-$	3.00 ± 0.08	3.14	2.85 ± 0.08	3.04	4.07	−0.027	1.08
$V_3Si_{11}^-$	3.02 ± 0.08	3.16	2.84 ± 0.08	3.08	4.09	−0.008	1.06
$V_3Si_{12}^-$	2.59 ± 0.08	2.54	2.44 ± 0.08	2.53	4.11	0.024	0.34
$V_3Si_{13}^-$	3.39 ± 0.08	3.41	3.07 ± 0.08	3.31	4.12	0.013	0.80
$V_3Si_{14}^-$	3.00 ± 0.2	3.34	2.90 ± 0.2	3.21	4.11		0.39

5.47 and 3.10 Å, respectively, and the cohesive energies for Si and V solids are 4.56 and 5.34 eV/atom, respectively. For comparison, the experimental lattice constants are 5.43 and 3.03 Å for Si and V solids, and the corresponding cohesive energies are 4.63 and 5.31 eV/atom, respectively.[63] In short, our PBE/DND scheme is able to describe the structural and bonding properties of V and Si systems in a satisfactory manner.

3. RESULTS AND DISCUSSION

3.1. Photoelectron Spectra of $V_3Si_n^-$ (n = 3−14) Clusters. Figure 1 displays the photoelectron spectra of $V_3Si_n^-$ clusters (n = 3−14) recorded with 266 nm (4.661 eV) photons. Each peak of the PES represents a transition from the ground state of the cluster anion to the ground or an excited state of their corresponding neutrals. To account for the broadening of the photoelectron spectra peaks due to the instrumental resolution, the ADE of each cluster was estimated by adding the value of the instrumental resolution to the electron binding energy at the crossing point between the baseline and the leading edge of the first peak. The VDE was estimated from the maximum of the first peak.

The spectrum of $V_3Si_3^-$ has a small peak at around 2.11 eV, which gives the VDE. After this, there is a broadened area and several peaks between 3 and 4 eV. The VDE of $V_3Si_4^-$ is about 2.51 eV. The front two peaks of the PES are close to each other, while the third one locates at about 3.5 eV. The spectrum of $V_3Si_5^-$ is similar to that of $V_3Si_4^-$ and the VDE is about 2.60 eV. For $V_3Si_6^-$, the first peak is very small and shows a little broadening, corresponding to a VDE of 2.46 eV. The successive five peaks become increasingly higher. The spectrum of $V_3Si_7^-$ exhibits a broad feature between 2.9 and 3.3 eV with three major peaks centered at 3.36, 3.66, and 3.95 eV. Four well-resolved peaks centered at 3.03, 3.44, 3.69, and 4.05 eV are evident in the spectrum of $V_3Si_8^-$. For $V_3Si_9^-$, there are two broad features at 3.2−3.4 eV and 3.5−4.1 eV plus a narrow peak at 3.88 eV. In the case of $V_3Si_{10}^-$, the intensity slowly increases from 3.0 to 3.9 eV and reaches a distinct peak at 3.9 eV. The PES of $V_3Si_{11}^-$ yields four peaks with increasing height. For the spectrum of $V_3Si_{12}^-$, a small broadened feature is seen from 2.5 to 3.0 eV and a peak appears over 4.0 eV. The first peak on the PES of $V_3Si_{13}^-$ emerges very late (at 3.39 eV), followed by a broadened area and a distinct peak at over 4.0 eV. For $V_3Si_{14}^-$, a small broadened feature around 3.00 eV (VDE) appears and several more peaks come out after 3.3 eV.

DOI: 10.1021/jp5112845
J. Phys. Chem. C 2015, 119, 10987−10994

All the VDEs and ADEs determined from photoelectron spectra in Figure 1 are summarized in Table 1. Overall speaking, VDE or ADE for a $V_3Si_n^-$ cluster increases with the number (n) of silicon atoms, whereas $V_3Si_6^-$ and $V_3Si_{12}^-$ show local minima. The detailed electronic properties will be discussed along with the theoretical calculations in section 3.3.

3.2. Low-Energy Structures of $V_3Si_n^-$ (n = 3−14) Clusters. The lowest-energy structures of $V_3Si_n^-$ (n = 3−14) clusters determined from GA-DFT global search are displayed in Figure 2, along with some important structural isomers for discussion. $V_3Si_3^-$-a has a C_s symmetry with V_3 triangle at the center and three Si atoms being separated on the two sides. The V−V bond lengths are 2.160, 2.160, and 2.656 Å, respectively. The BL of Si−Si is 2.657 Å and the average V−Si BL is 2.457 Å. The metastable one, $V_3Si_3^-$-b, which is 0.313 eV higher in energy, has an octahedral structure and there are only two V−V bonds (both are 2.087 Å). In the structure of $V_3Si_3^-$-c isomer, three Si atoms join together to form a line while three V atoms constitute a triangle.

In the ground state structure of $V_3Si_4^-$, four Si atoms constitute a polyline and three V atoms fill in the empty positions, forming a face-capped square bipyramid. The $V_3Si_4^-$-b isomer lies 0.115 eV higher in energy and has a bicapped triangle bipyramid configuration, in which three V atoms form a triangle at the center and four Si atoms are separated into two dimers. $V_3Si_4^-$-c is a pentagonal bipyramid with two V atoms on the vertex, while the rest one V and four Si atoms make up of a pentagon.

As the ground state, the geometry of $V_3Si_5^-$-a is a face-capped pentagonal bipyramid with slight distortion. The three V atoms form a triangle facet of the bipyramid, which is capped by a Si atom. In $V_3Si_5^-$-b isomer with ΔE = 0.206 eV, three V atoms and one Si atom constitute a quadrangle in the middle and the rest four Si atoms form two dimers and locate on the two sides. $V_3Si_5^-$-c structure consists of a square pyramid of Si_2V_3 and a Si_3 triangle and can be related to the most stable structure of $V_3Si_6^-$.

In $V_3Si_6^-$, three V atoms constitute a triangle with BL of 2.355 Å, 2.219 and 2.273 Å, respectively. This V_3 triangle forms the basal plane for a trigonal bipyramid with two Si atoms on top and bottom. Another trigonal bipyramid (VSi_4) is linked with this V_3Si_2 one by sharing one V atom. The entire cluster exhibits oblate geometry with C_s symmetry. The average V−V BL is 2.282 Å, shorter than the average BLs of 2.617 Å for V−Si and 2.448 Å for Si−Si.

In the lowest-energy $V_3Si_7^-$ anion cluster, three V atoms form an acute triangle, while an obtuse V_3 triangle is found in isomer $V_3Si_7^-$-b, which is 1.978 eV higher in energy. These two structures indeed resemble each other; both having a trigonal bipyramid of V_3Si_2 as a core surrounded by two and three Si atoms on the two sides.

In the most stable structure of $V_3Si_8^-$-a, eight Si atoms are separated into two parts (each form a four-atom rhombus) by the middle V_3 triangle. A more symmetric configuration (C_{2v}) is obtained as the metastable isomer $V_3Si_8^-$-b with ΔE = 0.108 eV. It can be viewed as an open trigonal bipyramid of V_3Si_2 in the middle capped with three Si atoms on each of the two sides. By capping one Si atom on the waist of $V_3Si_8^-$-b, the ground-state layered structure of $V_3Si_9^-$ anion is obtained. Similarly, $V_3Si_9^-$-b can be seen as placing a Si atom on the $V_3Si_8^-$-a with some reconstruction.

For the $V_3Si_{10}^-$ cluster, we found six low-lying isomers whose energy differences are in range of about 0.5 eV. $V_3Si_{10}^-$-a is a truncated V-centered icosahedron but with a hexagon instead of a pentagon on the bottom, whereas a distorted V-centered icosahedron ($V_3Si_{10}^-$-f) is 0.524 eV higher in energy. $V_3Si_{10}^-$-b, $V_3Si_{10}^-$-c, and $V_3Si_{10}^-$-d can all be constructed from $V_3Si_8^-$-a by adding two extra silicon atoms and fusing two parts. The 3−7−

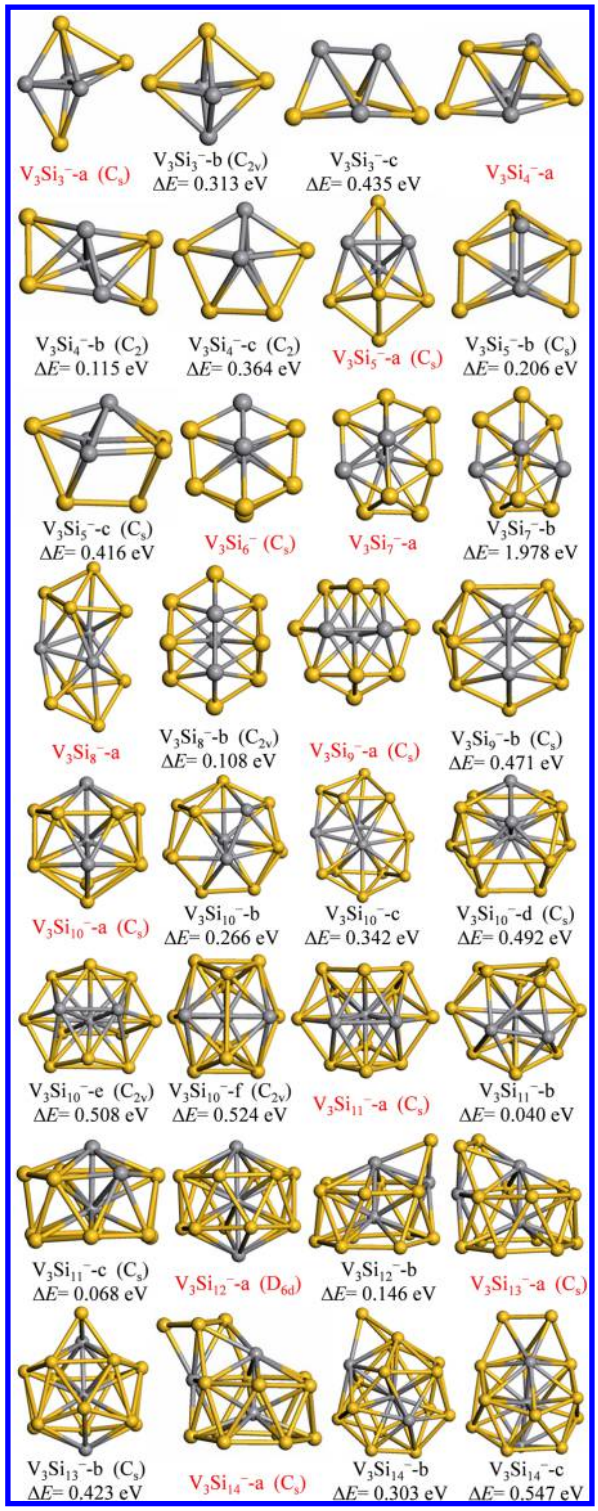

Figure 2. Low-energy structures of $V_3Si_n^-$ (n = 3−14) clusters. For each cluster size, the energy difference of several isomers (marked as $V_3Si_n^-$-b, $V_3Si_n^-$-c, and so on) with regard to the lowest-energy one (marked as $V_3Si_n^-$-a) are given by ΔE. The cluster symmetries are given in brackets (otherwise, C_1). Gray and yellow balls represent V and Si atoms, respectively.

DOI: 10.1021/jp5112845
J. Phys. Chem. C 2015, 119, 10987−10994

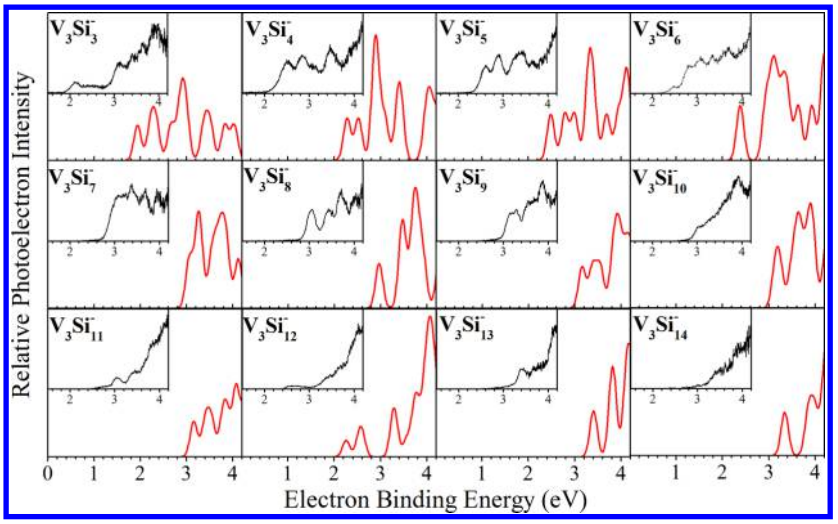

Figure 3. Photoelectron spectra for $V_3Si_n^-$ clusters (n = 3−14) from ab initio calculations. The insets are experimental data from Figure 1 for comparison. A uniform Gaussian broadening of 0.08 eV is chosen for all the simulated spectra.

3 layered configuration of $V_3Si_{10}^-$-e comes from $V_3Si_8^-$-b by capping two Si atoms on the back side, preserving C_{2v} symmetry.

The lowest-energy structure of $V_3Si_{11}^-$ is obtained by adding one Si atom to $V_3Si_{10}^-$-e, forming a 3−7−4 layered structure. With different arrangement of top five Si atoms, one can obtain a metastable structure of V_3Si_{11}-b with ΔE = 0.04 eV. Interestingly, $V_3Si_{11}^-$-c forms an incomplete V-center cage consisting of two hexagons (one with six Si atoms and the other with five Si atoms and one V atom) and one vertex V atom. This isomer is only less stable than the ground state by 0.068 eV.

As a continuation of $V_3Si_{11}^-$-c, the ground state configuration (D_{6d} symmetry) of $V_3Si_{12}^-$-a is composed of a central axis of V_3 surrounded by two staggered Si_6 hexagonal rings. This unique wheel-like structure has been reported in our recent publication.[48] Replacing one Si atom on the hexagonal ring by one V atom and capping this Si atom on the triangular face leads to the $V_3Si_{12}^-$-b isomer, whose energy is higher than the ground-state structure by 0.146 eV.

Starting from $V_3Si_{12}^-$-b, $V_3Si_{13}^-$-a can be constructed by further capping of an additional Si atom on the triangular face nearby the first capped Si atom. Capping one Si atom on the symmetric D_{6d} cage of $V_3Si_{12}^-$-a leads to $V_3Si_{13}^-$-b configuration; however, it is less stable by 0.423 eV probably due to distortion of the original 14-vertex cage.

$V_3Si_{14}^-$-a follows the structural motif of $V_3Si_{12}^-$-b and $V_3Si_{13}^-$-a, which can be obtained by capping one additional Si atom on the upper lateral Si_2V triangle of $V_3Si_{13}^-$-a. $V_3Si_{14}^-$-b is a severely distorted V-centered cage face capped with one Si atom. Isomer $V_3Si_{14}^-$-c can be viewed as adding two Si atoms on $V_3Si_{12}^-$-a; however, the two additional Si atoms leads to significant deviation from the original D_{6d} symmetry of $V_3Si_{12}^-$-a cage.

Overall speaking, in the low-lying structures of $V_3Si_n^-$ (n = 3−14) clusters, vanadium atoms tend to bond with each other and form V_3 triangle since V−V bond is stronger than V−Si bond, with the only exception at $V_3Si_{12}^-$-a. For all $V_3Si_n^-$ clusters considered, the lengths of V−V bonds are in the range of 2.160−2.656 Å, moderately shorter than BLs of V−Si (2.360−2.695 Å) and Si−Si (2.414−2.657 Å). The smaller $V_3Si_n^-$ clusters, with n = 3−9 adopt flat-shape, while incomplete cages with one V atom at the center form at $V_3Si_{10}^-$ and $V_3Si_{11}^-$. A highly symmetric V-centered D_{6d} cage emerges at $V_3Si_{12}^-$, which also exhibits interesting ferrimagnetic behavior (magnetic moments on V atoms: 2.4 μ_B, −0.6 μ_B, and 2.4 μ_B, respectively).[48] The ground state structures of $V_3Si_{13}^-$ and $V_3Si_{14}^-$ can be obtained by capping Si atoms on the D_{6d} cage of $V_3Si_{12}^-$ with the bottom atom truncated.

The present structural motifs of $V_3Si_n^-$ clusters can be compared to the silicon clusters doped with one or two vanadium atoms. In the case of VSi_n clusters, 12 Si atoms are needed to completely surround the central vanadium atom, while open basket structures are preferred for n < 12. So far, little is known for the growth pattern of V_2Si_n clusters. For $V_2Si_{12}^-$ cluster,[48] our recent PES combined DFT study revealed a structure with 12 Si atoms forming a hexagonal antiprism cage, one V atom in the cage center, and another V on the top. It was theoretically predicted that tube-like double hexagonal prism structure with some distortion is most stable for V_2Si_{18} cluster.[44] At last, V_2Si_{20} cluster has an elongated dodecahedron configuration with a V_2 unit encapsulated inside Si_{20} cage, which is the smallest fullerene-like silicon cage.[47] Even with limited knowledge on the V_2Si_n clusters, it seems that coexistence of three vanadium atoms in the silicon framework results in different structural pattern with regard to those with only one or two vanadium dopants. Therefore, doping three or more transition metal atoms into silicon clusters would lead to new opportunities in tailoring the structural and electronic properties of the doped silicon clusters.

3.3. Electronic Properties of $V_3Si_n^-$ (n = 3−14) Clusters with Ground-State Structures. Based on the energy levels of anionic clusters, photoelectron spectra were simulated using the "generalized Koopman's theorem".[64] A nonvanishing energy shift of the energy levels is required for describing the asymptotic Kohn−Sham equations. With broadening the shifted energy levels, it provides a simple and efficient way to obtain the photoelectron spectra from the density of states. Generally, this viable method yields a faithful description of the experimental data, although it has ignored the true excited states of a cluster. Figure 3 displays the simulated photoelectron spectra for the lowest structures of $V_3Si_n^-$ clusters (n = 3−14) in Figure 2, along with the experimental spectra in Figure 1 for comparison. One can see satisfactory overall agreement

DOI: 10.1021/jp5112845
J. Phys. Chem. C 2015, 119, 10987−10994

between simulated and measured spectra, demonstrating the validity of the present theoretical approaches.

For $V_3Si_3^-$, the simulated spectrum shows four discrete peaks and a broad one. Except for the first one that is different from the experimental results, the others agree well. In the simulated spectrum of $V_3Si_4^-$, it also has four main peaks as observed in the experimental PES, while the fifth peak comes out at 4.05 eV. Compared to experiment, the overall spectrum is slightly narrower and moved forward in energy. For $V_3Si_5^-$, the first peak locates at 2.48 eV and the following peak is broadened into two peaks. The essential characteristics of experimental PES are excellently reproduced by DFT calculation. In the simulated spectrum of $V_3Si_6^-$, the first two peaks are separated by a big valley while these peaks merge together in experimental spectrum. For $V_3Si_7^-$, a relatively narrower feature and two major peaks at 3.25 and 3.79 eV are obtained in the simulated spectrum. Such three-peak behavior is also seen in experiment. Similarly, three major peaks can be clearly found in the theoretical spectrum of $V_3Si_8^-$ except for a small shift of ~0.1 eV compared to the experimental data. The simulated spectrum of $V_3Si_9^-$ presents the same tendency as the experimental one. The DFT simulation successfully reproduces the experimental trend and yields three obvious peaks at 3.19, 3.55, and 3.89 eV, except for a dip at 3.36 eV. For the PES of $V_3Si_{11}^-$, both DFT calculation and experiment yield four peaks with increasing height. The existing difference between theory and experiment might be attributed to the limited distinguish ability in experiment. Similar three-peak and two-peak behaviors occur in the $V_3Si_{13}^-$ and $V_3Si_{14}^-$ clusters, respectively. For the simulated PES of $V_3Si_{12}^-$, five peaks are centered at 2.24, 2.58, 3.30, 3.79, and 4.06 eV, respectively. The former two overlap with each other and the fourth one shows as a shoulder of the fifth peak. In short, we suspect that the discrepancy between theory and experiment is due to the limited experimental resolution, which leads to overlap of several peaks into a broad feature.

To further explore the electronic properties of $V_3Si_n^-$ clusters, the measured and computed vertical detachment energies (VDEs) and adiabatic detachment energies (ADEs) of the cluster anions are plotted in Figure 4. In the experimental curve of VDEs, one can find an increasing trend from 2.0−3.4 eV, except for the local minima at $V_3Si_6^-$, $V_3Si_{12}^-$, and $V_3Si_{14}^-$. The theoretical VDEs reproduce this trend generally well, whereas there is a noticeable overestimation (0.34 eV) at $V_3Si_{14}^-$. In general, the ADE of a cluster anion is equal to the adiabatic electron affinity (EA) of the corresponding neutral species when their geometries are close to each other. From experiment, one can find that ADE keep rising from 1.9−2.2 eV for $V_3Si_n^-$ (n = 3−6) and this trend becomes slowly in the range of 2.7−3.0 eV as the number of silicon atoms increases from 7 to 11. Afterward, the ADE shows an odd−even oscillation from n = 11 to 14, with a local minimum at $V_3Si_{12}^-$ (2.44 ± 0.08 eV). Again, the experimental tendency is well reproduced by ab initio simulation, with an overestimation of about 0.27 eV at $V_3Si_{13}^-$ and $V_3Si_{14}^-$. In both ADE and VDE, $V_3Si_{12}^-$ shows a distinct minimum with regard to its neighboring sizes. From both geometric and electronic points of view, $V_3Si_{12}^-$ stands out as a unique species with high symmetry and appreciable stability. For a given neutral cluster, the lower EA corresponds to higher stability. In other words, V_3Si_{12} neutral cluster is stable. The details of this fascinating cluster have already been discussed in our recent publication.[48]

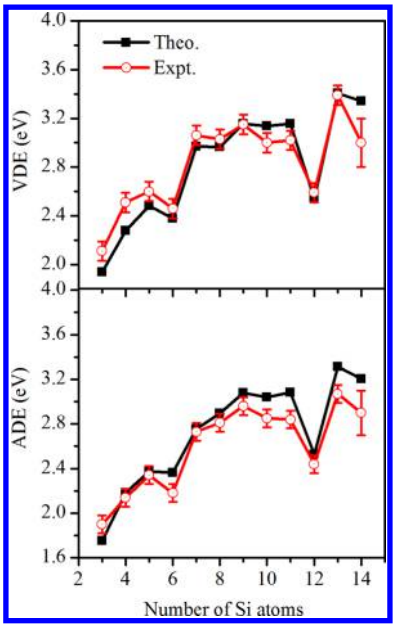

Figure 4. Vertical detachment energies (VDEs) and adiabatic detachment energies (ADEs) of $V_3Si_n^-$ clusters: black squares, theory; red circles, experiment.

3.4. Stabilities and HOMO−LUMO Gaps of $V_3Si_n^-$ (n = 3−14) Clusters. In Figure 5a, we plot the binding energies of $V_3Si_n^-$ clusters as a function of size n. For a A_xB_y cluster, its binding energy is defined by $E_b(A_xB_y) = (E(A_xB_y) - xE(A) - yE(B))/(x + y)$, where $E(A_xB_y)$ is the energy of A_xB_y cluster, $E(A)$ or $E(B)$ is the energy per single atom of element A or B in the vacuum, x or y is the number of A or B atoms in the cluster. The binding energy gradually increases with growing number of Si atoms, suggesting the formation of a cluster is more and more easy as it becomes bigger. To examine the relative stability, the second order energy differences (Δ_2E) of the clusters in their ground-state geometries are calculated and plotted in Figure 5b. One can see three peaks at $V_3Si_5^-$, $V_3Si_9^-$, and $V_3Si_{12}^-$, indicating that they are more stable than their neighboring sized clusters. The high stability of $V_3Si_{12}^-$ can be related to its high symmetry, closed cage configuration, and lower VDE or ADE.

As shown in Figure 5c, the HOMO−LUMO gaps of $V_3Si_n^-$ clusters range between 0.4 and 1.2 eV. $V_3Si_4^-$, $V_3Si_{10}^-$, and $V_3Si_{11}^-$ possess relatively higher gaps while the gaps of $V_3Si_6^-$, $V_3Si_{12}^-$, and $V_3Si_{14}^-$ are lower. We also compare these gap values to the pure neutral silicon clusters with same total number of atoms from DFT calculations, whose amplitudes are between 0.86 and 2.21 eV.[65] On average, replacing three Si atoms by V atoms reduces the gap by ~1.1 eV.

4. CONCLUSIONS

Using a linear time-of-flight mass spectrometer and a magnetic-bottle photoelectron spectrometer, we generated $V_3Si_n^-$ (n = 3−14) clusters in a laser vaporization source and recorded their photoelectron spectra. Meanwhile, using an unbiased genetic algorithm, we globally searched the low-energy structures of these $V_3Si_n^-$ clusters. For each cluster, the three V atoms tend to form triangle surrounded by Si atoms. Accordingly, the average length of V−V bonds of about 2.3 Å is 0.3 Å shorter than that of V−Si. An exception case was found at $V_3Si_{12}^-$, which has a wheel-like D_{6d} structure with a central V_3 axis and

DOI: 10.1021/jp5112845
J. Phys. Chem. C 2015, 119, 10987−10994

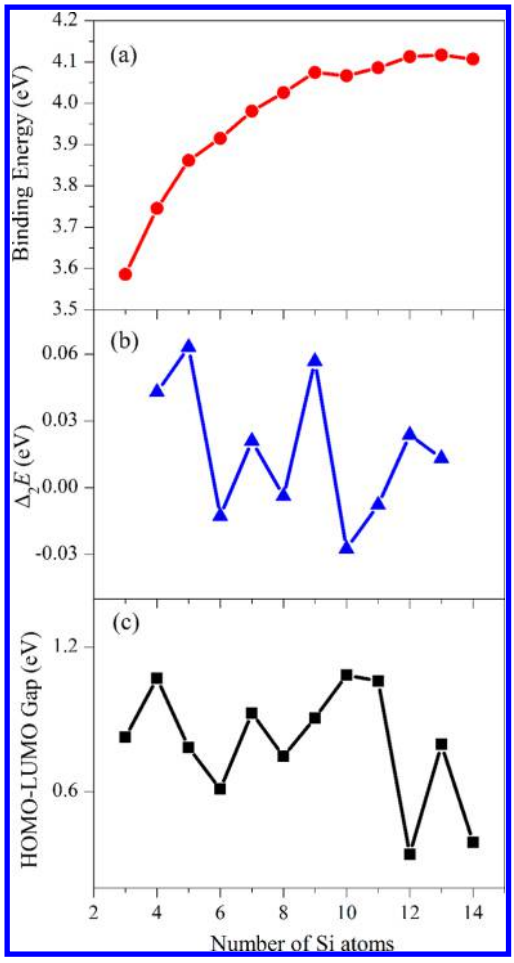

Figure 5. Binding energies (a), second-order of energy differences (Δ_2E) (b), and HOMO−LUMO gaps (c) of $V_3Si_n^-$ (n = 3−14) clusters.

exhibits ferrimagnetism. The agreement of PES, ADE, and VDE between experiments and theoretical calculations are satisfactory. In particular, the size-dependent trends of ADE and VDE are well reproduced by ab initio calculations, confirming that we have located the correct ground state configurations of these $V_3Si_n^-$ clusters.

AUTHOR INFORMATION

Corresponding Authors

*Phone: +86-411-84709748. E-mail: zhaojj@dlut.edu.cn.

*Phone: +86-10-62564816. E-mail: xuhong@iccas.ac.cn.

Notes

The authors declare no competing financial interest.

ACKNOWLEDGMENTS

This work was supported by the Knowledge Innovation Program of the Chinese Academy of Sciences (Grant No. KJCX2-EW-H01) and the National Natural Science Foundation of China (Grant No. 21103202, 11134005, 20853001, and 11304030).

REFERENCES

(1) Kumar, V. *Nanosilicon*; Elsevier: Amsterdam, Netherlands, 2011.

(2) Baletto, F.; Ferrando, R. Structural properties of nanoclusters: Energetic, thermodynamic, and kinetic effects. *Rev. Mod. Phys.* **2005**, *77*, 371−423.

(3) Raghavachari, K.; Rohlfing, C. M. Bonding and stabilities of small silicon clusters: A theoretical study of Si_7−Si_{10}. *J. Chem. Phys.* **1988**, *89*, 2219−2234.

(4) Röthlisberger, U.; Andreoni, W.; Parrinello, M. Structure of nanoscale silicon clusters. *Phys. Rev. Lett.* **1994**, *72*, 665−668.

(5) Ho, K.-M.; Shvartsburg, A. A.; Pan, B.; Lu, Z.-Y.; Wang, C.-Z.; Wacker, J. G.; Fye, J. L.; Jarrold, M. F. Structures of medium-sized silicon clusters. *Nature* **1998**, *392*, 582−585.

(6) Lu, Z.-Y.; Wang, C.-Z.; Ho, K.-M. Structures and dynamical properties of C_n, Si_n, Ge_n, and Sn_n clusters with n up to 13. *Phys. Rev. B* **2000**, *61*, 2329.

(7) Zhu, X.; Zeng, X. Structures and stabilities of small silicon clusters: Ab initio molecular-orbital calculations of Si−Si. *J. Chem. Phys.* **2003**, *118*, 3558−3570.

(8) Zhu, X.; Zeng, X.; Lei, Y.; Pan, B. Structures and stability of medium silicon clusters. II. Ab initio molecular orbital calculations of Si−Si. *J. Chem. Phys.* **2004**, *120*, 8985−8995.

(9) Zdetsis, A. D. High-symmetry high-stability silicon fullerenes: A first-principles study. *Phys. Rev. B* **2007**, *76*, 075402.

(10) Kumar, V.; Kawazoe, Y. Metal-encapsulated fullerenelike and cubic caged clusters of silicon. *Phys. Rev. Lett.* **2001**, *87*, 045503.

(11) Kumar, V. Alchemy at the nanoscale: Magic heteroatom clusters and assemblies. *Comput. Mater. Sci.* **2006**, *36*, 1−11.

(12) Neukermans, S.; Wang, X.; Veldeman, N.; Janssens, E.; Silverans, R. E.; Lievens, P. Mass spectrometric stability study of binary MS_n clusters (S = Si, Ge, Sn, Pb, and M = Cr, Mn, Cu, Zn). *Int. J. Mass Spectrom.* **2006**, *252*, 145−150.

(13) Hiura, H.; Miyazaki, T.; Kanayama, T. Formation of metal-encapsulating Si cage clusters. *Phys. Rev. Lett.* **2001**, *86*, 1733−1736.

(14) Koyasu, K.; Akutsu, M.; Mitsui, M.; Nakajima, A. Selective Formation of MSi_{16} (M = Sc, Ti, and V). *J. Am. Chem. Soc.* **2005**, *127*, 4998−4999.

(15) Claes, P.; Janssens, E.; Ngan, V. T.; Gruene, P.; Lyon, J. T.; Harding, D. J.; Fielicke, A.; Nguyen, M. T.; Lievens, P. Structural identification of caged vanadium doped silicon clusters. *Phys. Rev. Lett.* **2011**, *107*, 173401.

(16) Lu, J.; Nagase, S. Structural and electronic properties of metal-encapsulated silicon clusters in a large size range. *Phys. Rev. Lett.* **2003**, *90*, 115506.

(17) Wang, J.; Zhao, J.; Ma, L.; Wang, G.; King, R. B. Stability and magnetic properties of Fe encapsulating in silicon nanotubes. *Nanotechnology* **2007**, *18*, 235705.

(18) Khanna, S. N.; Rao, B. K.; Jena, P. Magic numbers in metallo-inorganic clusters: Chromium encapsulated in silicon cages. *Phys. Rev. Lett.* **2002**, *89*, 016803.

(19) Janssens, E.; Lievens, P. Growth mechanisms for doped clusters. *Adv. Nat. Sci: Nanosci. Nanotechnol.* **2011**, *2*, 023001.

(20) Kumar, V.; Kawazoe, Y. Magic behavior of $Si_{15}M$ and $Si_{16}M$ (M = Cr, Mo, and W) clusters. *Phys. Rev. B* **2002**, *65*, 073404.

(21) Ma, L.; Zhao, J.; Wang, J.; Lu, Q.; Zhu, L.; Wang, G. Structure and electronic properties of cobalt atoms encapsulated in Si_n (n = 1−13) clusters. *Chem. Phys. Lett.* **2005**, *411*, 279−284.

(22) Uchida, N.; Miyazaki, T.; Kanayama, T. Stabilization mechanism of Si_{12} cage clusters by encapsulation of a transition-metal atom: A density-functional theory study. *Phys. Rev. B* **2006**, *74*, 205427.

(23) Bandyopadhyay, D.; Kumar, M. The electronic structures and properties of transition metal-doped silicon nanoclusters: A density functional investigation. *Chem. Phys.* **2008**, *353*, 170−176.

(24) Wang, J.; Ma, Q.-M.; Xu, R.-P.; Liu, Y.; Li, Y.-C. 3d transition metals: Which is the ideal guest for Si_n cages? *Phys. Lett. A* **2009**, *373*, 2869−2875.

(25) Kawamura, H.; Kumar, V.; Kawazoe, Y. Growth behavior of metal-doped silicon clusters Si_nM (M = Ti, Zr, Hf; n = 8−16). *Phys. Rev. B* **2005**, *71*, 075423.

(26) Kawamura, H.; Kumar, V.; Kawazoe, Y. Growth, magic behavior, and electronic and vibrational properties of Cr-doped Si clusters. *Phys. Rev. B* **2004**, *70*, 245433.

DOI: 10.1021/jp5112845
J. Phys. Chem. C 2015, 119, 10987−10994

(27) Janssens, E.; Gruene, P.; Meijer, G.; Wöste, L.; Lievens, P.; Fielicke, A. Argon physisorption as structural probe for endohedrally doped silicon clusters. *Phys. Rev. Lett.* **2007**, *99*, 063401.
(28) Kong, X.; Xu, H.-G.; Zheng, W. Structures and magnetic properties of $CrSi_n^-$ (n = 3−12) clusters: Photoelectron spectroscopy and density functional calculations. *J. Chem. Phys.* **2012**, *137*, 064307.
(29) Wang, J.; Zhao, J.; Ma, L.; Wang, B.; Wang, G. Structure and magnetic properties of cobalt doped clusters. *Phys. Lett. A* **2007**, *367*, 335−344.
(30) Torres, M. B.; Fernández, E. M.; Balbás, L. C. Structure and relative stability of Si_n, Si_n^-, and doped Si_nM clusters (M = Sc^-, Ti, V^+) in the range n = 14−18. *J. Comput. Meth. Sci. Eng.* **2007**, *7*, 241−256.
(31) Bandyopadhyay, D. A density functional theory based study of the electronic structures and properties of cage like metal doped silicon clusters. *J. Appl. Phys.* **2008**, *104*, 084308.
(32) Yang, A. P.; Ren, Z.-Y.; Guo, P.; Wang, G.-H. Geometries, stabilities, and electronic properties of Y-doped Si_n (n = 1−16) clusters: A relativistic density functional investigation. *J. Mol. Struct. (THEOCHEM)* **2008**, *856*, 88−95.
(33) Jaiswal, S.; Babar, V. P.; Kumar, V. Growth behavior, electronic structure, and vibrational properties of Si_nY anion clusters (n = 4−20): Metal atom as linker and endohedral dopant. *Phys. Rev. B* **2013**, *88*, 085412.
(34) Furuse, S.; Koyasu, K.; Atobe, J.; Nakajima, A. Experimental and theoretical characterization of MSi_{16}^-, MGe_{16}^-, MSn_{16}^-, and MPb_{16}^- (M = Ti, Zr, and Hf): The role of cage aromaticity. *J. Chem. Phys.* **2008**, *129*, 064311.
(35) Zheng, W.; Nilles, J. M.; Radisic, D.; Bowen, K. H. Photoelectron spectroscopy of chromium-doped silicon cluster anions. *J. Chem. Phys.* **2005**, *122*, 071101.
(36) Koyasu, K.; Atobe, J.; Akutsu, M.; Mitsui, M.; Nakajima, A. Electronic and geometric stabilities of clusters with transition metal encapsulated by silicon. *J. Phys. Chem. A* **2007**, *111*, 42−49.
(37) Koyasu, K.; Atobe, J.; Furuse, S.; Nakajima, A. Anion photoelectron spectroscopy of transition metal- and lanthanide metal−silicon clusters: MSi_n^- (n = 6−20). *J. Chem. Phys.* **2008**, *129*, 214301.
(38) Ohara, M.; Koyasu, K.; Nakajima, A.; Kaya, K. Geometric and electronic structures of metal (M)-doped silicon clusters (M = Ti, Hf, Mo, and W). *Chem. Phys. Lett.* **2003**, *371*, 490−497.
(39) Xu, H.-G.; Zhang, Z.-G.; Feng, Y.; Yuan, J.; Zhao, Y.; Zheng, W. Vanadium-doped small silicon clusters: Photoelectron spectroscopy and density-functional calculations. *Chem. Phys. Lett.* **2010**, *487*, 204−208.
(40) Claes, P.; Ngan, V. T.; Haertelt, M.; Lyon, J. T.; Fielicke, A.; Nguyen, M. T.; Lievens, P.; Janssens, E. The structures of neutral transition metal doped silicon clusters, Si_nX (n = 6−9; X = V, Mn). *J. Chem. Phys.* **2013**, *138*, 194301.
(41) Xu, H.-G.; Wu, M. M.; Zhang, Z.-G.; Yuan, J.; Sun, Q.; Zheng, W. Photoelectron spectroscopy and density functional calculations of $CuSi_n^-$ (n = 4−18) clusters. *J. Chem. Phys.* **2012**, *136*, 104308.
(42) Kong, X.-Y.; Deng, X.-J.; Xu, H.-G.; Yang, Z.; Xu, X.-L.; Zheng, W.-J. Photoelectron spectroscopy and density functional calculations of $AgSi_n^-$ (n = 3−12) clusters. *J. Chem. Phys.* **2013**, *138*, 244312.
(43) Han, J.-G.; Zhao, R.-N.; Duan, Y. Geometries, stabilities, and growth patterns of the bimetal Mo_2-doped Si_n (n = 9−16) clusters: A density functional investigation. *J. Phys. Chem. A* **2007**, *111*, 2148−2155.
(44) Ji, W.; Luo, C. Structures, magnetic properties, and electronic counting rule of metals-encapsulated cage-like M_2Si_{18} (M = Ti−Zn) clusters. *Int. J. Quantum Chem.* **2012**, *112*, 2525−2531.
(45) Ji, W.-X.; Luo, C. Density-functional investigation of hexagonal prism transition-metal-encapsulated cage M_2Si_{18} (M = Sc−Zn) clusters. *Model. Simul. Mater. Sci. Eng.* **2010**, *18*, 025011.
(46) Xu, H.-G.; Zhang, Z.-G.; Feng, Y.; Zheng, W. Photoelectron spectroscopy and density-functional study of $Sc_2Si_n^-$ (n = 2−6) clusters. *Chem. Phys. Lett.* **2010**, *498*, 22−26.
(47) Xu, H. G.; Kong, X. Y.; Deng, X. J.; Zhang, Z. G.; Zheng, W. J. Smallest fullerene-like silicon cage stabilized by a V_2 unit. *J. Chem. Phys.* **2014**, *140*, 024308.
(48) Huang, X.; Xu, H.-G.; Lu, S.; Su, Y.; King, R. B.; Zhao, J.; Zheng, W. Discovery of a silicon-based ferrimagnetic wheel structure in $V_xSi_{12}^-$ (x = 1−3) clusters: Photoelectron spectroscopy and density functional theory investigation. *Nanoscale* **2014**, *6*, 14617−14621.
(49) Deaven, D. M.; Ho, K. M. Molecular geometry optimization with a genetic algorithm. *Phys. Rev. Lett.* **1995**, *75*, 288−291.
(50) Zhao, J. J.; Xie, R. H. Genetic algorithms for the geometry optimization of atomic and molecular clusters. *J. Comput. Theor. Nanosci.* **2004**, *1*, 117−131.
(51) Delley, B. An all-electron numerical method for solving the local density functional for polyatomic molecules. *J. Chem. Phys.* **1990**, *92*, 508−517.
(52) Delley, B. From molecules to solids with the $DMol^3$ approach. *J. Chem. Phys.* **2000**, *113*, 7756−7764.
(53) Perdew, J. P.; Burke, K.; Ernzerhof, M. Generalized gradient approximation made simple. *Phys. Rev. Lett.* **1996**, *77*, 3865−3868.
(54) Sai, L.; Tang, L.; Zhao, J.; Wang, J.; Kumar, V. Lowest-energy structures and electronic properties of Na-Si binary clusters from ab initio global search. *J. Chem. Phys.* **2011**, *135*, 184305.
(55) Sai, L.; Zhao, J.; Huang, X.; Wang, J. Structural evolution and electronic properties of medium-sized gallium clusters from ab initio genetic algorithm search. *J. Nanosci. Nanotechnol.* **2012**, *12*, 132−137.
(56) Huang, X.; Sai, L.; Jiang, X.; Zhao, J. Ground state structures, electronic and optical properties of medium-sized Na_n^+ (n = 9, 15, 21, 26, 31, 36, 41, 50, and 59) clusters from ab initio genetic algorithm. *Eur. Phys. J. D* **2013**, *67*, 1−7.
(57) Sai, L.; Tang, L.; Huang, X.; Chen, G.; Zhao, J.; Wang, J. Lowest-energy structures of $(WO_3)_n$ ($2 \le n \le 12$) clusters from first-principles global search. *Chem. Phys. Lett.* **2012**, *544*, 7−12.
(58) Hong, L.; Wang, H.; Cheng, J.; Huang, X.; Sai, L.; Zhao, J. Atomic structures and electronic properties of small Au−Ag binary clusters: Effects of size and composition. *Comput. Theor. Chem.* **2012**, *993*, 36−44.
(59) Spain, E. M.; Behm, J. M.; Morse, M. D. The 846 nm $A'^3\Sigma^{-u} \leftarrow X^3\Sigma^{-g}$ band system of jet-cooled V_2. *J. Chem. Phys.* **1992**, *96*, 2511−2516.
(60) Huber, K. P.; Herzberg, G. *Constants of Diatomic Molecules*; Van Nostrand Reinhold: New York, 1979.
(61) James, A. M.; Kowalczyk, P.; Langlois, E.; Campbell, M. D.; Ogawa, A.; Simard, B. Resonant two photon ionization spectroscopy of the molecules V_2, VNb, and Nb_2. *J. Chem. Phys.* **1994**, *101*, 4485−4495.
(62) Winstead, C. B.; Paukstis, S. J.; Gole, J. L. Spectroscopy of the $H^3\Sigma^{-u}$ electronic state of Si_2 using a combined laser vaporization-REMPI and oven-based LIF study. *J. Mol. Spectrosc.* **1995**, *173*, 311−332.
(63) Kittel, C. *Introduction to Solid State Physics*, 8 ed.; Wiley: New York, 1996; Vol. 7.
(64) Akola, J.; Manninen, M.; Häkkinen, H.; Landman, U.; Li, X.; Wang, L.-S. Photoelectron spectra of aluminum cluster anions: Temperature effects and ab initio simulations. *Phys. Rev. B* **1999**, *60*, R11297−R11300.
(65) Wei, Q.; Lu, W.-C.; Zhao, L.-Z.; Zang, Q.-J.; Wang, C. Z.; Ho, K. M. Stabilities and fragmentation energies of Si_n clusters (n = 2−33). *J. Phys.: Condens. Matter* **2009**, *21*, 455501.

DOI: 10.1021/jp5112845
J. Phys. Chem. C 2015, 119, 10987−10994